

# Demonstration of Metrics for Self-Healing and Self-Reconfiguration in a Monolithic and Segmented Robotic System

Jaxson Hill\*, Griffin MacRae†, Pierson Lintala‡, and Noah Taniguchi§  
*University of Southern California, Los Angeles, CA 90089*

Joshua Pastizzo¶  
*University of Southern California, Los Angeles, CA 90089*  
*Johns Hopkins University, Baltimore, MD 21218*

Ethan Bootehsaz||, Harrison Pearl\*\*, Charlene Yuen††, David Samia‡‡, Le Duong§§, Niccolo Von-Bueren¶¶, Tyler Rotello\*\*\*, Wei-Min Shen†††, and David A. Barnhart†††  
*University of Southern California, Los Angeles, CA 90089*

## I. Introduction

Failures in robotic systems are inevitable given a sufficiently large time scale. Although one can design to maximize the system lifespan or minimize risk of mission failure, it is necessary for robotic systems to be fault-tolerant and capable of recovering performance once a failure occurs. This fact is made more important when these robotic systems operate in environments where humans cannot readily repair or maintain the systems, such as in and beyond low Earth orbit. Therefore, it is necessary to consider how a generic robotic system can detect its own failures, determine an appropriate response, and then execute a sequence of actions to restore performance.

This paper defines two such ways to restore performance: traditional redundancy and self-healing. Redundancy we define to be situations in which a failure in a component or subsystem can be overcome by use of extra and identical hardware. Examples may be having more Inertial Measurement Units (IMU) than necessary to determine the inertial state of the system or having more limbs than necessary to produce any locomotion. In contrast, self-healing or self-reconfiguration involves the system modifying its physical configuration to minimize performance loss after a failure. In this case, when a failure occurs, there may not be extra and identical hardware to continue in the failed component's place. Instead, existing components may be repurposed or reconfigured to continue performing the task at hand. A theoretical example of this type of behavior may be altering the configuration of segments in a robotic arm to maintain the range of motion and execution of a specific task of the arm.

In order to gauge and compare the relative benefits of a system equipped with the ability to self-heal, a system of metrics is required to take objective measurements of self-healing outcomes. This is required to generalize the concepts of self-healing across robotic systems with generic morphologies, and to provide inputs to any risk assessments done when considering the addition of self-healing capabilities to a system. In this paper, we propose a set of metrics to be generally applicable and adaptable to analyze the healing capabilities of any robotic system. Select metrics are then used to analyze two morphologically opposite robotic systems as a case study to demonstrate and utilize self-healing

---

\*PhD Student, Space Engineering Research Center, University of Southern California. Correspond to jthill@usc.edu.

†Research Engineer, Space Engineering Research Center.

‡Research Engineer, Space Engineering Research Center.

§Graduate Student, Department of Astronautical Engineering.

¶Research Engineer, Space Engineering Research Center. Graduate Student, Department of Electrical and Computer Engineering, AIAA Young Professional.

||Graduate Student, Department of Computer Science.

\*\*Graduate Student, Department of Computer Science.

††Graduate Student, Department of Computer Science.

‡‡Graduate Student, Department of Computer Science.

§§Graduate Student, Department of Computer Science.

¶¶Graduate Student, Department of Computer Science.

\*\*\*Graduate Student, Department of Computer Science.

†††Associate Professor, Department of Computer Science.

††††Research Director, Space Engineering Research Center. Research Professor, Department of Astronautical Engineering

techniques and measures of success. Each system will heal from an imposed failure in one of the degrees of freedom, then the performance is analyzed under the proposed framework to consider the effects of the heal.

## II. Self-Healing Metrics

The following is a proposed list of measures by which elements of a self-healing process may be objectively analyzed and compared between systems or design iterations. When designing a system with self-healing abilities in mind, it is necessary to consider which criteria are most relevant for the specific task or set of tasks at hand.

Metric	Definition
Post-Healing Performance Efficiency	The ratio of restored functionality to the original functionality of the robot after self-healing
Healing Adaptability	The robot's ability to heal from different types of damages or adapt its healing process based on the nature and extent of the damage. Proportion of total failure modes for which a healing strategy exists.
Post-Healing Durability and Maximum Healing Cycle	The longevity and performance of the robot after undergoing self-healing, measured by the number of successive heals the robot accomplishes before the self-healing strategy fails.
Detection Accuracy and Self-Diagnosis Capability	The precision with which the robot can identify and locate the cause of the failure driving healing, measured by proportion of possible failures correctly identified.
Healing Cost	The opportunity cost, in time, power, sacrificed ability, or other relevant quantity, to perform a healing action.
Detection time	The time it takes for a robot to detect damage and initiate the self-healing process.
Recovery Speed	The time it takes for a robot to start and complete a healing action.

Table 1 Key metrics for evaluating self-healing in robotic systems.

## III. Representative Robotic Systems Overview

Two robotic systems were selected to demonstrate the implementation of self-healing principles. These two systems were selected as they are morphologically distinct and were therefore useful in showing the applicability of self-healing principles on systems of varying architectures. The first system REACCH, is a "monolithic" robotic system whereby a discrete number of subsystems assemble to form the robotic system as a whole. The second system, SuperBot, is a "segmented" system consisting of an indefinite number of identical 3DOF modules to assemble and reassemble into varying forms. Both systems are expanded upon further below.

### A. Monolithic System Design - REACCH

REACCH is a bio-inspired robotic gripper equipped with silicone pads for the soft capture of orbital space debris of any size, shape, and configuration [1]. The silicone pad substrate has a rough texture applied to it to increase its effective shear load. The robotic arms are configured to mechanically conform to large/irregular objects to ensure that all the pads are applied in shear. In this configuration, self-healing elements have been added to enable repositioning of the arms in the event of a DOF failure in the system.

### B. Segmented System Design - SuperBot

Modular self-reconfigurable robots consist of multiple identical units capable of rearranging their connectivity to adapt to new tasks or recover from damage. The SuperBot system is one such design, featuring Lego-like autonomous modules that can form various morphologies (e.g., snake, crawler, arm) and even perform self-repair [2]. Each module is an independent 3-DOF robot with its own power, sensors, and six androgynous docking faces, allowing any module to connect to any other. An improved genderless connector called SINGO ("Single-End-Operative and Genderless") was

introduced to ensure a connection can be made or broken even if one side is unresponsive, a key enabler for self-healing [3]. This paper presents a segmented modular robotic system built from SuperBot modules and demonstrates self-healing reconfiguration after module failures. The system comprises two robot arms that can detach or recombine modules autonomously using SINGO docking mechanisms.

Each SuperBot module (Figure 1) is a roughly 100mm cube-shaped segment housing control electronics and motors, with androgynous SINGO docking interfaces on multiple faces. The modular arms are constructed by linking modules in series for each arm. The two arms are mounted on a common platform in a segmented configuration, effectively creating a dual-arm robot where each arm can function independently or dock with the other. Androgynous SINGO connectors [3] allow any module to attach to any other from either side, and importantly, enable a functional module to disconnect a failed neighbor (since only one side needs to actuate the latch). This design ensures that a “stuck” connection will not permanently seize the robot’s configuration if one module fails. The segmented architecture provides inherent redundancy: the system can isolate a faulty segment and re-route connectivity via the remaining modules.

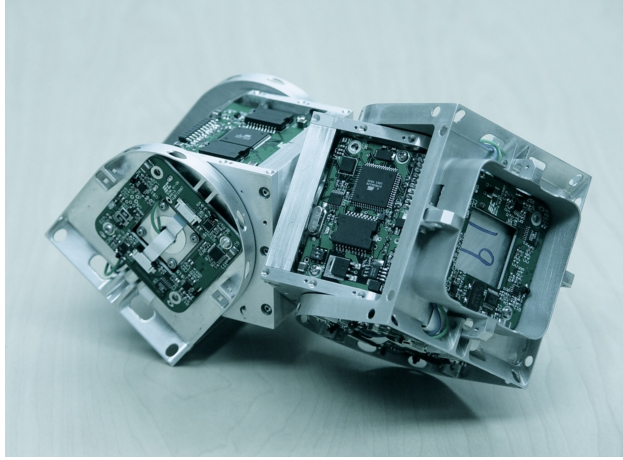


**Fig. 1 Segmented Design: SuperBot Module Close-Up.**

The hardware testbed (Figure 2) shows the two arms constructed from SuperBot units. White tubular link housings are used to secure the modules and represent fixed-length segments between module joints. Each arm (labeled Arm 1 and Arm 2) is connected to a flat support platform at its base. The design parameters are illustrated in the schematic diagram of Figure 3. Arm 1 has  $n$  modules and Arm 2 has  $m$  modules (in the tested configuration,  $n = 2$  and  $m = 3$ ). Each module has length  $l$ , and additional link segments of length  $s$  (the white housings) can be used to extend reach. The two arm bases are separated by a distance  $d$  on the platform. A failure of a base module (index 0) is considered a worst-case scenario, potentially severing the arm’s attachment to the platform at an angle  $\theta$ . The system is designed such that the other arm can dock to the free end of a broken arm or otherwise support it during reconfiguration.

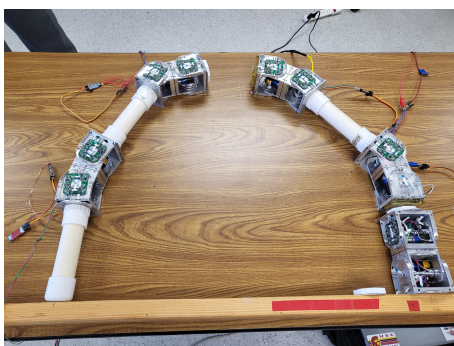


**Fig. 2 Segmented Design: Segmented Arm Hardware Testbed**

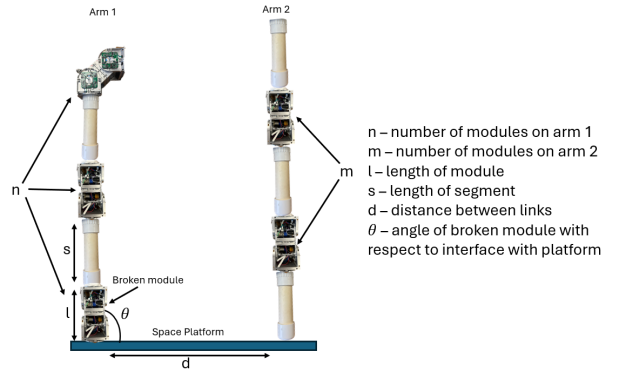


**Fig. 3 Segmented Design: System Layout and Parameters**

## IV. Self Healing Demonstrations

### A. Monolithic Healing Demonstration

REACCH was augmented to incorporate self-healing functions in the event of damage or loss of control to one or more of the arms. With the addition of the self-healing mechanisms, there are three degrees of freedom within each arm: arm position, arm rotation, and arm flexion. As described earlier, the arms are placed on lockable rotating bearings attached to lockable sliders along a circular track. While this implementation is actuated manually, the premise can be expanded to be mechanized and automated.

In its "nominal" state, REACCH has 4 arms, each placed 90° apart from each other around the circle. To demonstrate and measure self-healing, a representative locking failure of one arm was prescribed - one arm was kept in its curled up, unactuated state which is notated as the "unhealed" configuration. The remaining three arms were then repositioned along the circular track to each be 120° apart to create the "healed" configuration, thus resuming symmetry to the system. Tests were performed in the nominal, unhealed, and healed configuration to measure gripping performance to determine the post-healing performance efficiency, as defined in Table 1. As the system is a robotic gripper, the performance metrics chosen were maximum weight held and engagement with each segment of the arm.

Tests were conducted by suspending REACCH above a table and placing an 0.8 m diameter inflated ball on a fixed mount beneath the center of REACCH. REACCH was lowered to a fixed height, commanded to grab the ball, then lifted back up to hold the ball in the air. Known weight was gradually added to the bottom of the ball until the grip failed and the ball slipped, giving the maximum held weight for that configurations. Tests were done in all three configurations, and, for the unhealed and healed configurations, multiple trials were done using each arm as the "dead" arm, to control for any unique behavior for an individual arm. Engagement data was collected through the entire sequence by force sensing resistor sensors beneath each silicone gripping surface.

Healing adaptability is to be measured by demonstrating a healing scenario under every type of degree of freedom failure in the system. An example scenario is seen in Figures 4 and 5.

Duplicated grab tests are also being developed in PyChrono to attempt to replicate results in simulated environments.

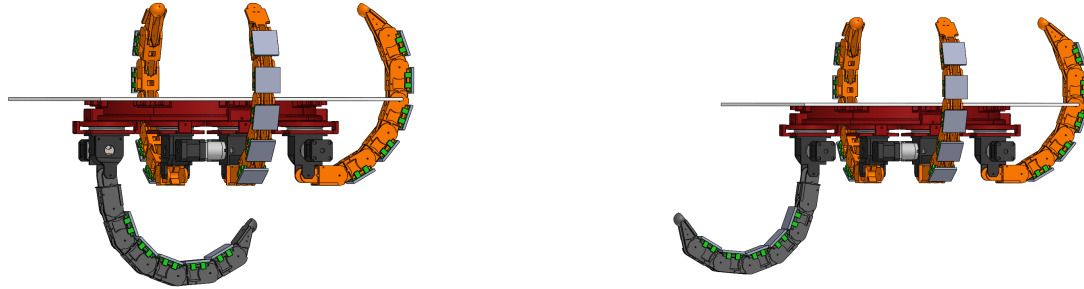


**Fig. 4** The grey arm has failed in a locked position inward, blocking capture of an object

**Fig. 5** The pivot rotates the dead arm outward, restoring performance

### B. Simulation-Based Segmented Healing Demonstration

We developed a physics-based simulation to validate the self-healing reconfiguration strategy. The simulation models each SuperBot module as a link with rotational joints and simulates the SINGO docking actions. We concentrated on the base failure case (module 0 on Arm 1) as a representative worst-case. Upon detecting the base module failure, the control algorithm executes a sequence of actions to restore connectivity:

- **Recovery Docking:** Arm 2 (the healthy arm) is commanded to move its tip to the free end of Arm 1. Using the SINGO dock, Arm 2's tip module actively docks with the interface on Arm 1's first module. This creates a continuous structure bridging Arm 1 to Arm 2, bypassing the failed base.
- **Failure Isolation:** The joint connecting the failed base module to Arm 1 is unlocked, detaching the rest of Arm 1 from the base module (the failed module stays attached to the platform but is now separated from the rest of the arm).
- **Reconfiguration:** With the new connection made, Arm 1's modules are now supported by Arm 2. The combined structure reorients and attaches to the platform via Arm 2's base. Essentially, Arm 2 assumes the role of the base

for Arm 1's modules.

- **Restoration:** The system has effectively “healed” by removing the faulty base and reconnecting Arm 1 to the platform through Arm 2. The robot can continue operation, albeit with a modified configuration (one arm now longer, attached through the other arm).

The simulation sequence (Figure 6) shows four key frames of the simulation. Additional simulations (not shown here) have been conducted for failures at other module positions (e.g., mid-arm module 1 or end module 2) and for different arm length configurations. Ongoing simulation studies are examining the full range of failure indices and various arm separation distances  $d$  to ensure the robustness of the approach in all permutations.

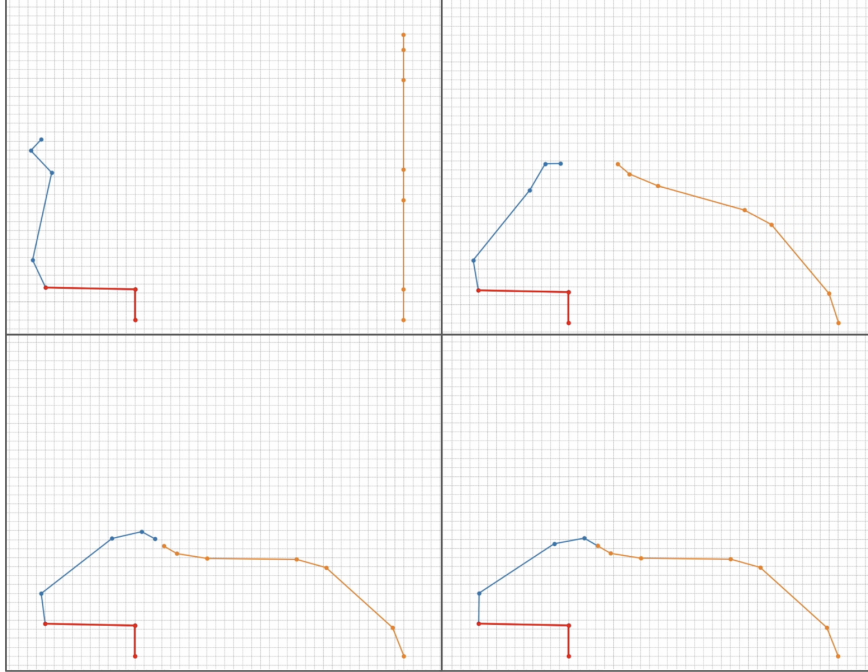


**Fig. 6 Simulated Recovery from a Base (Module 0) Failure.** Top left to bottom right: (1) initial state with Arm 1 (blue) attached to the platform via module 0 (red) and Arm 2 (orange) upright; (2-3) Arm 2 approaches and docks with Arm 1's free end; (4) Arm 1 detaches from its failed base (red) and is free; Arm 2's base now anchors both arms, completing the reconfiguration.

### C. Real-World Segmented Healing Demonstration

To validate the approach in hardware, we performed an autonomous docking and reconfiguration experiment using the dual-arm SuperBot testbed. In this demonstration, one arm is programmed to simulate a failure at its base, and the other arm is autonomously controlled to perform the healing steps. The modules coordinate over a wireless network, and each module's microcontroller runs a distributed docking algorithm to align and connect the SINGO interfaces.

Figure 7 captures a sequence of four stages during the failure isolation and docking process. In the top-left image, the two arms are initially individually attached to the platform. The base of Arm 1 (right side of arch) is then signaled as “failed.” Top-right: Arm 2 pivots its tip toward Arm 1's tip. Arm 2's tip successfully docks with the module at Arm 1's tip. Bottom-left: Arm 1's base module disengages its connection to the rest of the arm, allowing Arm 2 to begin pulling away. Bottom-right: Arm 2 successfully moves away. Arm 1's remaining modules are now supported by the connection to Arm 2. Throughout this sequence, the system used on-board sensing (infrared proximity and mechanical alignment guides) to achieve reliable docking without human intervention.

After docking and removing the working modules, the robot proceeds to reintegrate Arm 1 to the platform. Figure 8 shows these subsequent steps. – in essence, the robot has performed a self-healing operation. This demonstration confirmed that the SINGO connectors and control logic work in practice: the modules successfully executed the mechanical docking maneuvers and passed control from one arm to the other. The entire sequence was completed autonomously, showcasing a practical self-reconfiguration in hardware. Full automation of alignment (using sensor

feedback) was a key challenge observed, and improvements in docking precision are ongoing to reduce the time and retries needed for physical connection.

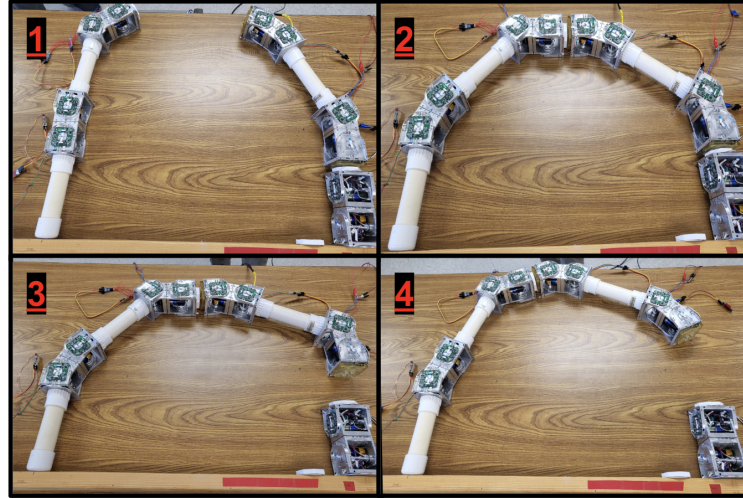


**Fig. 7 Docking and Detachment Sequence**

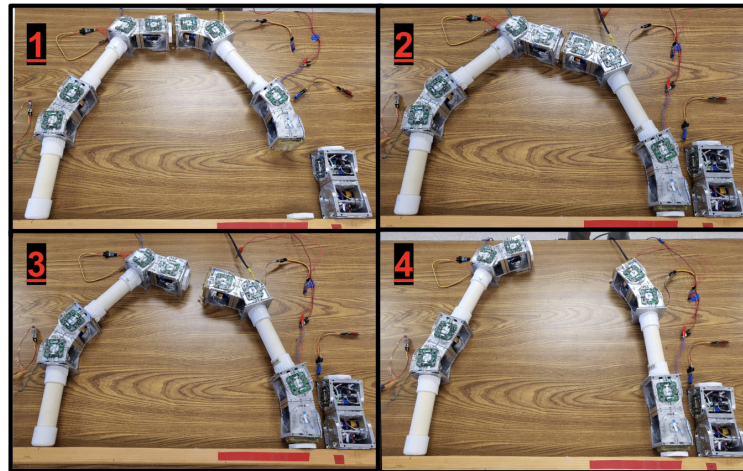


**Fig. 8 Reconnection and Undocking Sequence.**

**Top-left:** the combined arm structure (Arms 1+2 connected) begins to move as a single unit. **Top-right:** the merged arm adjusts its configuration to bring Arm 1 back down to the platform mounting point and Arm 1 is re-attached to the platform, effectively restoring it to service with one less module. **Bottom-left:** Arm 2 then undocks from Arm 1, returning to its original attachment point on the platform. **Bottom-right:** The end result is that Arm 1 is reattached to the platform minus the failed base module, and Arm 2 has returned to its normal position

## V. Preliminary Results

### A. Monolithic Results

Results demonstrated that the "healed" configuration of the monolithic design exhibited improved weight performance compared to the "unhealed" system. In measuring the post-healing performance efficiency, the healed configuration supported 32% more weight than the unhealed configuration; the unhealed configuration held, on average, 57% of the nominal system's weight while the healed configuration held, on average, 76% of the nominal system's weight. Figure 9 shows a box plot and plot with the mean and one standard deviation for each configuration.

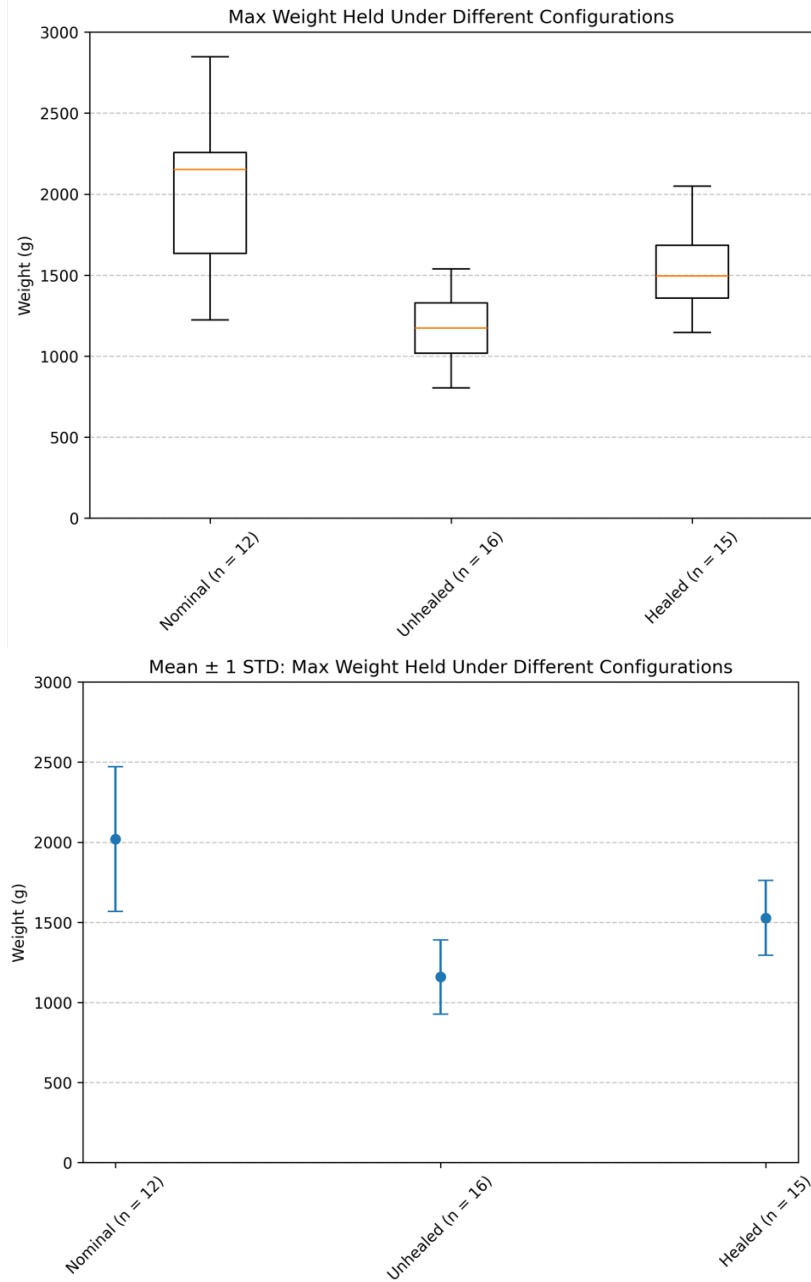


**Fig. 9 Monolithic Design: Max Weight Results**

Preliminary results indicate that while the healed configuration showed an increase in average force engagement along the length of the limb compared to the unhealed configuration, there was no substantial increase in the overall

percent engagement of each individual link. This is seen in Figure 10 and Figure 11.

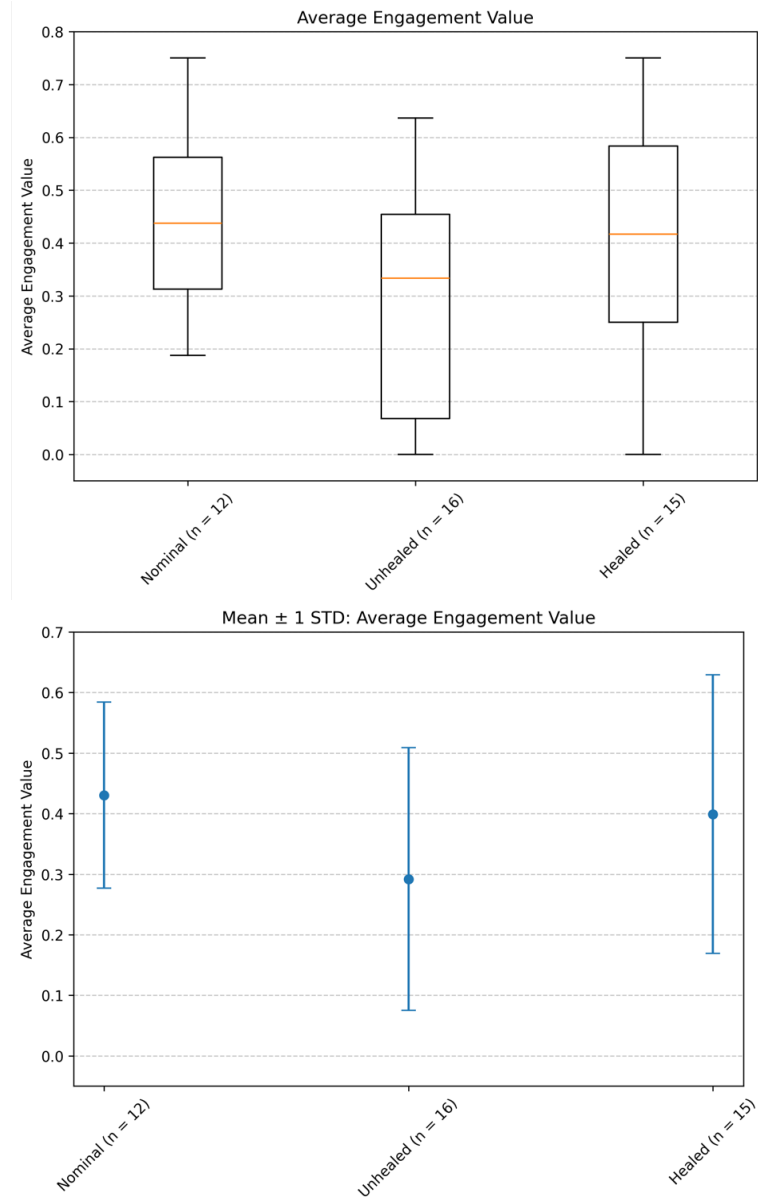


**Fig. 10 Monolithic Design: Average Engagement Results**

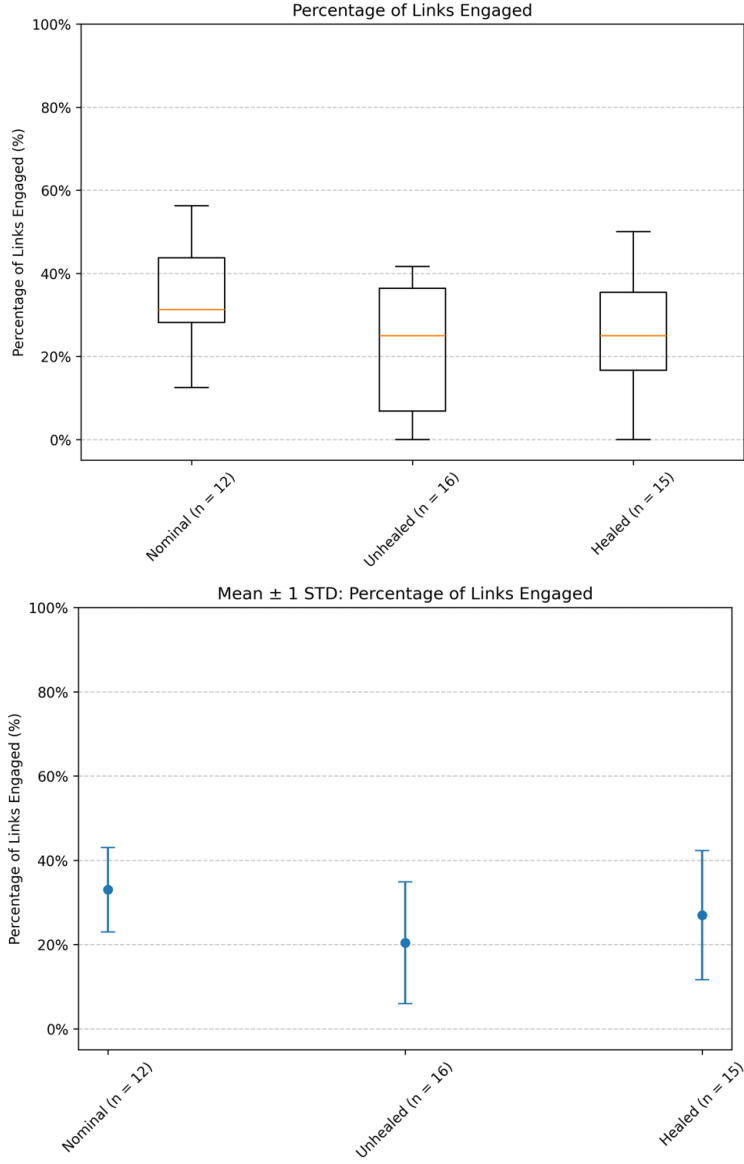


**Fig. 11 Monolithic Design: Percent Engagement Results**

## B. Segmented Results

The ability of the segmented system to heal was evaluated under varying module failure angles, module indices, and arm ratios. For each combination of module index and arm ratio, the percent of scenarios that could heal from the initial failure angle was measured and recorded as the healing adaptability metric, as defined in 1. A trial was counted as a success if the algorithm managed to either remove the failed module or bypass it and end with at least one continuous 5-DOF arm (out of the original 6-DOF) capable of reaching an end effector. If the modules ended up in a stalemate (unable to dock or reconnect), or if the arm remained split, it was a failure. Dozens of simulation trials were run for each combination of failure location and arm ratio.

Figure 12 summarizes the healing success probability for each failure location across varying distances. Here, the arm ratio represents the normalized base distance as previously defined.

The results clearly illustrate:

- Base module (index 0) failures present the most significant recovery challenge, particularly at larger distances (), with success rates sharply decreasing to near 0%.
- Middle (index 1) and tip (index 2) module failures exhibit consistently high recovery success rates (80–100%)

across most tested distances, with only minor reductions at the extreme distances () .

This quantitative analysis confirms that segmented robotic systems significantly enhance healing adaptability, particularly for failures occurring away from the base. Understanding these recovery limitations and success patterns directly informs robotic arm design decisions and control strategies. For instance, designers might reinforce or provide redundancy at base modules, while control systems could prioritize avoiding known angles where the configuration is not healable and pursue reconfiguration strategies that exploit distal module flexibility.

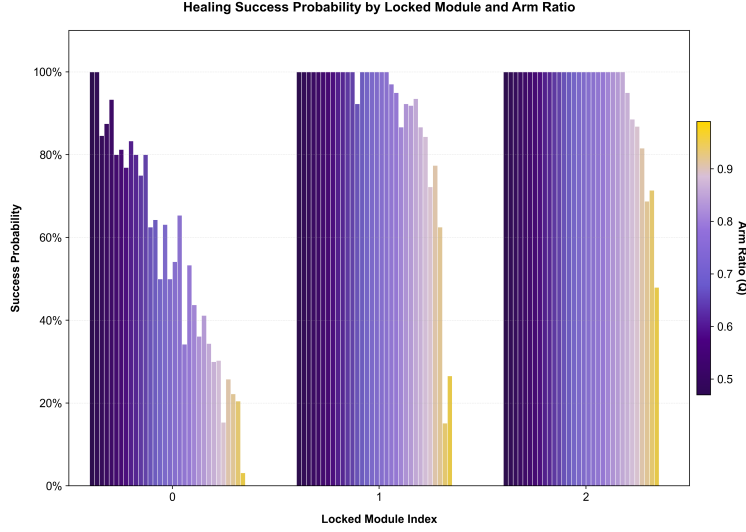


**Fig. 12 Simulated Healing Success vs. Failure Position and Arm Ratio**

## VI. Limitations and Future Work

While the current demonstration showcases the potential of self-healing in a segmented robot arm, there are several limitations to acknowledge, along with planned future improvements. First, all experiments on the SuperBot system have been conducted in a quasi-2D planar setup. The simulation constrained the arms to move in a plane, and the real hardware was operated on a flat table with essentially planar motion (the arms mainly rotated in the horizontal plane to dock). This 2D approach simplifies the docking problem (as the modules only needed to align yaw rotation, not roll/pitch in 3D space). However, real-world applications will require full 3D self-reconfiguration. In 3D, modules could approach from arbitrary orientations, making the alignment problem more complex. Future work will involve extending our control algorithms to handle 3D docking orientations. This includes using the SuperBot's multiple docking faces – for instance, a module could approach and attach from above or below, not just head-on in the same plane. We will leverage the module's built-in IMUs and perhaps vision sensors to aid 3D alignment. The transition from 2D to 3D reconfiguration will also necessitate more sophisticated planning algorithms to decide the approach vector and to avoid collisions in space.

Additionally, there is future work to extend the simulation of the segmented system docking to cover all permutations of the design variables in Figure 3. We plan to incorporate additional sensing and adaptive control to handle misalignment and to automate reattachment for any location of failure with the goal to generalize the self-healing capability to arbitrary configurations and module networks, enabling modular robots to withstand multiple failures sequentially by reconfiguring themselves. This capability is a step toward autonomous systems with extreme robustness: robots that can survive and continue their mission despite losing components. Our results so far demonstrate the feasibility of a self-repairing robotic architecture using real hardware modules.

For REACCH, there are current limitations around the amount of available limbs with which to demonstrate self-healing and measure how performance degrades with loss of each arm. With additional data, determining a correlation between healed and unhealed performance and amount of limbs may be possible. Additionally, the team plans to further explore to what extent the added self-healing capabilities enable healing adaptability. Fully measuring against all single point and double point failures, then mapping each degree of freedom failure to a probability of that joint failing, could inform trade studies for future monolithic robotic systems on whether adding additional joints to heal

increases or decreases the overall risk of mission failure in a system.

In both systems, the team plans to explore the application of other metrics to analyze the system. Expanding the scope and demonstration of the metrics is key to furthering the ideas of self-healing into foreign systems.

## VII. Conclusion

Preliminary conclusions indicate the applicability and validity of applying self healing metrics across diverse robotic architectures. When eventual failure and degradation of components are assumed to be true, it is important to consider comparison and self-healing analysis techniques to ensure maximum probability of mission success and to replenish capabilities with mission performance is diminished.

## VIII. Acknowledgements

The authors would like to acknowledge and thank Kall Morris Inc. for use of information regarding their REACCH module.

## References

- [1] Narayanan, S., Barnhart, D., Rogers, R., Ruffatto, D., Schaler, E., Van Crey, N., Dean, G., Bhanji, A., Bernstein, S., Singh, A., et al., “REACCH-Reactive electro-adhesive capture cloth mechanism to enable safe grapple of cooperative/non-cooperative space debris,” *AIAA Scitech 2020 Forum*, 2020, p. 2134.
- [2] Salemi, B., Moll, M., and Shen, W.-m., “SUPERBOT: A Deployable, Multi-Functional, and Modular Self-Reconfigurable Robotic System,” *2006 IEEE/RSJ International Conference on Intelligent Robots and Systems*, 2006, pp. 3636–3641. <https://doi.org/10.1109/IROS.2006.281719>.
- [3] Shen, W.-M., Kovac, R., and Rubenstein, M., “SINGO: a single-end-operative and genderless connector for self-reconfiguration, self-assembly and self-healing,” *2009 IEEE international conference on robotics and automation*, IEEE, 2009, pp. 4253–4258.